Did the Samalas Volcano Eruption in 1257 Initiate Climate Change That Resulted in LIA (Little Ice Ages)? Statistical Study of Global Climate Proxy Data since 1000

Ika Umratul Asni Aminy
Institut Teknologi Bandung
Satria Bijaksana (satria@fi.itb.ac.id)
Institut Teknologi Bandung https://orcid.org/0000-0001-6374-4128
Darharta Dahrin
Institut Teknologi Bandung

Research Article

Keywords: Little Ice Age, Samalas Volcano, Glaciers, Descriptive Statistics, Inferential Statistics, Northern Hemisphere

Posted Date: March 8th, 2022

DOI: https://doi.org/10.21203/rs.3.rs-1422056/v1

Did the Samalas Volcano Eruption in 1257 Initiate Climate Change That Resulted in LIA (Little Ice Ages)? Statistical Study of Global Climate Proxy Data since 1000

Ika Umratul Asni Aminy, Satria Bijaksana*, Darharta Dahrin

Faculty of Mining and Petroleum Engineering, Institut Teknologi Bandung, Jalan Ganesa 10, Bandung 40132, Indonesia

*Corresponding author: satria@fi.itb.ac.id

Abstract

The Little Ice Age (LIA) describes cold conditions that lasted for centuries associated with the expansion of glaciers that could be initiated by a large volcanic eruption. The 1257 eruption of the Samalas volcano caused climatic impacts worldwide and possibly has played a role in starting the LIA. The injected volcanic material was so extraordinary that statistically significant results were obtained. To test whether the Samalas eruption triggered climate change that resulted in LIA, the data used in this study refers to 7 curves of temperature reconstruction in the Northern Hemisphere because they are formed based on multi-proxy data. Furthermore, data processing is carried out in 4 stages, namely selecting the temperature reconstruction curve for the years 1000-2000, digitizing the curve, interpolating, and normalizing the temperature value. The data is then selected first based on the similarity of the shape of the digitization curve, the results of descriptive statistics are in accordance with the LIA periodization, and the results of inferential statistics show that there is no difference in temperature between the data. Based on the results obtained, the trend curve of temperature changes at 50-year intervals from each data group in the Northern Hemisphere can show global climate

change due to the Samalas eruption and prove that the eruption of Samalas initiated climate change which resulted in LIA.

Keywords: Little Ice Age; Samalas Volcano; Glaciers; Descriptive Statistics; Inferential Statistics; Northern Hemisphere

Introduction

Paleoclimatology is the study of climate based on natural phenomena that can provide proxy data records to determine climate changes that occur on Earth (Bradley 2015). Early studies of past climate change relied on evidence of environmental changes commonly observed in mountainous regions of the world (Matthes 1939; Bradley and Jones 1993). Such observations prompted Matthes (1939) to introduce the term Little Ice Age (LIA). The LIA describes time lapses associated with glacier expansion in various regions (Matthes 1939; Matthews and Briffa 2005; Olivia 2018). The cooling phase of LIA begins at high latitudes, then extends across the region with different intensities and periods (Paasche and Bakke 2010; Olivia 2018). The period characterized by the LIA generally ranges from 1550 to 1850 (Bradley and Jones 1992). However, the lack of instrumental data available in various regions causes proxy data to be more widely used to determine climate change that occurs.

Volcanic eruptions can affect climate depending on the amount and height of the injected volcanic material (Rampino and Self 1982; Hansen et al. 1992; McCormick et al. 1995; Morita et al. 2005; Miller et al. 2012; Raible et al. 2016). Larger volcanic eruptions, such as the 1991 eruption of Pinatubo, cause global climate variations for 2 to 3 years after the eruption (Morita et al. 2005). Aerosol movement and atmospheric dynamics from the Pinatubo eruption can be detected and measured by satellite observations to accurately

determine the mechanism and impact caused by the explosion (McCormick et al. 1995). In addition, the Tambora eruption in April 1815 also had a major impact on the global climate (Rampino and Self 1982; Morita et al. 2005; Raible et al. 2016) and caused a “year without a summer” in Europe and North America in 1816 (Morita et al. 2005). The Pinatubo and Tambora eruptions can provide a big picture of the impact of volcanic eruptions on climate change on Earth. The impact of climate change due to large-scale volcanic eruptions in the future (2090-2100) will be more dangerous than in the past (1990-2000), this is related to the injection of volcanic material due to changes in troposphere elevation that produce a stratosphere layer temperature anomaly that continues to increase even until the 3rd year after the eruption, causing an increase in albedo, a reduction in the radiation force, and cooling of the Earth (Aubry et al. 2021).

Large volcanic eruptions could cause tremendous impacts. Mount Samalas in 1257 was suspected as the main cause of climate change which resulted in LIA. This is related to sulfur deposits in the ice core due to the eruption which reached twice that of the Tambora eruption (Lavigne et al. 2013). In addition, a prolonged shift in climate to cooler temperatures also occurred in the 13th century, especially after the Samalas eruption (Gennaretti et al. 2014). These conditions indicate that the volcanic material injected from the Samalas eruption is so extraordinary that it is possible to obtain statistically significant results. Statistical processing refers to temperature reconstruction curves from the proxy data set to prove whether the Samalas eruption triggered climate change that resulted in LIA. The use of multi-proxy data can reduce the weakness of each indicator so that more accurate results can be obtained (McGregor et al. 2010) compared to the results of studies that only use one type of proxy data.

Data and Methods

In this study, the data used refers to 7 curves of temperature reconstruction in the Northern Hemisphere (Figure 1) from several previously published research results with details as shown in Table 1. This data was chosen because the temperature reconstruction curve was formed based on multi-proxy data. The use of only one type of proxy data (tree rings) cannot show a globally consistent cooling response after the Samalas eruption (Büntgen et al. 2022). In addition, the Northern Hemisphere also tends to show more accurate temperature reduction results than the Southern Hemisphere (Briffa et al. 1998; Raible et al. 2016; Aubry et al. 2021). The obtained temperature reconstruction curves have different year intervals. Therefore, to facilitate statistical processing, the data must have the same year range, namely 1000-2000 years with a difference of 10 years. The temperature reconstruction curve is then digitized to get the temperature value for each data. If the digitization year position does not match the desired year position, it is necessary to do interpolation (*I*) to get the correct value using the following formula.

$$I = \frac{Ia - Ib}{Xa - Xb}(Xx - Xb) + Ib \quad (1)$$

where, Ia = temperature value (upper limit), Ib = temperature value (lower limit), Xx = year when temperature value is desired, Xa = year value (upper limit) and Xb = year value (lower limit).

Furthermore, the temperature value data needs to normalize into the range 0-1. It aims to equalize the values obtained so that there is no data inequality during statistical tests.

$$N = \frac{y_i - y_{min}}{y_{max} - y_{min}} \quad (2)$$

where, y_i = temperature value at point i, y_{min} = smallest temperature value and y_{max} = largest temperature value.

Digital curve shapes before and after interpolation and normalization need to be compared to find out that the interpolated and normalized data obtained already reflect accurate data. Thus, the same curve shape of the comparison results can show that the data after interpolation and normalization correspond to the reference curve (temperature reconstruction curve from a previously published study) used. Furthermore, to prove the Samalas eruption triggered the climate change that resulted in the LIA, the data must show the global impact of the explosion. The data is determined based on the obtained digital curve shape. In this study, the same curve pattern is shown to show the global climate influence due to the Samalas eruption. In addition, the determination of the data is also done based on the processing of descriptive and inferential statistics. At this stage the processing carried out refers to the previous results (curve shape). If the resulting curve does not match or has a different shape from the others, it will be removed and not used in further statistical processing (descriptive and inferential).

Descriptive statistical processing presents data in the form of a curve that refers to the interaction between the mean (mean value) of the normalized temperature of each data with the LIA periodization. This processing uses the Statistical Package for the Social Sciences (SPSS) to see whether the data used (7 data from the Northern Hemisphere) can show that the coldest period (lowest temperature) occurred in the LIA period (1550-1850), then the period after the eruption (1260-1540) caused by climatic disturbances due to the Samalas eruption. Meanwhile, the pre-eruption period (1000-1250) and post-LIA (1860-2000) represent the condition of each data without global influence due to the Samalas eruption.

Processing of inferential statistics using SPSS and manual calculations to determine whether there is a difference in temperature between the data. Inferential statistical test using Two

Way Analysis of Variance (ANOVA) because it refers to the data obtained in this study. ANOVA test can be applied if the data is quantitative, normally distributed, and homogeneous. Therefore, the normality test uses the Chi-Square formula (χ^2), while to determine the homogeneity of the data it is carried out using the Levene (W) formula.

$$\chi^2 = \frac{(f_o - f_h)^2}{f_h} \quad (3)$$

where, f_o= frequency/amount of observational data, and f_h = expected frequency/amount (percentage of the area of each field multiplied by the amount of data)

$$W = \frac{(n-k)\sum_{i=1}^{k} n_i(\bar{Z}_i - \bar{Z})^2}{(k-1)\sum_{i=1}^{k}\sum_{j=1}^{k}(Z_{ij} - \bar{Z}_i)^2} \quad (4)$$

where, k = number of data groups, n = number of data, $\bar{Z}_i$ = average value of Z per group, $\bar{Z}$ = average value of Z overall and Z_{ij} is Z value per group defined as

$$Z_{ij} = \left|Y_{ij} - \bar{Y}_i\right| \quad (5)$$

where, Y_{ij} = value of each data and $\bar{Y}_i$ = average value of the group to i

If one of the requirements of the ANOVA test is not met, then the Friedman test (χ_r^2) is carried out to determine the effect of temperature between data.

$$\chi_r^2 = \frac{12}{nk(k+1)}\sum_{j=1}^{k} R_j^2 - 3n(k+1) \quad (6)$$

where, R_j^2 = total rank squared, k = number of data groups, and n = number of data

If the Friedman test results show a difference in temperature values, it is necessary to carry out the Tukey's Honest Significance Difference (HSD) test (Abdi and Williams 2010). The Tukey test is needed because the Friedman test results cannot explain which data is different or the same, while the Tukey test results can explain it.

$$HSD = q_{A,\ \alpha}\sqrt{\frac{MS_{S(A)}}{S}} \quad (7)$$

where, $q_{A,\ \alpha}$ = the value obtained from the Tukey HSD value table, S = number of data,

and $MS_{S(A)}$ is the mean square of error.

Inferential statistical data showing global effects due to the Samalas eruption (no temperature difference) is used to show events related to climate phenomena that occurred, especially to prove whether the eruption of Samalas initiated climate change that resulted in LIA. At this stage, a curve is formed using SPSS based on changes in the normalized mean temperature values of all data in each group at 50-year intervals, where the 1250-1300 year-range is heavily disturbed by volcanism (Brewington 2016). So, the data used starts from 1010 to 1960 with an interval of 50 years to see the trend of temperature changes that occur.

Results and Discussion

The data used in this study refers to 7 curves of temperature reconstruction in the Northern Hemisphere. The obtained curves were digitized to get the temperature and year values from all data. However, the digitization results cannot be processed because they have varying values (difference between temperature and year values in the data). Therefore, the data obtained are interpolated first by referring to the upper and lower limits of the temperature value and the year of digitization. Then the temperature value data is normalized so that there is no discrepancy in the data in the statistical test.

The shape of the digitization curve before and after interpolation and normalization shows the same results (Figure 2), although the data used refers to different values. The initial digital curve (before interpolation) is formed based on various data intervals, while the curve after interpolation and normalization refers to uniform data (1000-2000 years with a difference of 10 years). These results indicate that the data obtained after interpolation and normalization

175 correspond to the reference curve used in this study. Furthermore, the data is selected in
176 advance to determine data that accurately describes the global climate effects due to the
177 Samalas eruption. Data selection was determined based on the shape of the digitizing curve
178 (Figure 2a-2g), descriptive statistical results (Figure 3), and inferential (Tables 2 and 3) based
179 on the normalized mean temperature value.
180
181 Based on the digitized results that have been interpolated and normalized, the shape of the
182 curve (Figure 2a-2g) shows a similar pattern of change, this may be because the temperature
183 reconstruction curve is built based on multi-proxy data to produce accurate data. The shape of
184 the curve shows a decrease in temperature after the Samalas eruption and continues to
185 decrease as the LIA period approaches, although sometimes it increases but still cannot return
186 to normal conditions (conditions before the Samalas eruption). However, temperature
187 conditions began to return and even experienced a significant increase as the 20th century
188 approached.
189
190 Based on the shape of the curve obtained, all data show the same curve pattern. Therefore,
191 the data is reused in the processing of descriptive statistics. The results of the descriptive
192 statistical curve show the response of the normalized average temperature value to the LIA
193 periodization which is suitable for all data (Figure 3), where the LIA period shows the coldest
194 conditions due to a decrease in temperature for centuries. Then followed the period after the
195 Samalas eruption because H_2SO_4 from the Samalas eruption caused more sunlight to be
196 reflected into space, resulting in a decrease in Earth's temperature. However, the period
197 before the Samalas eruption and post-LIA represents the regional conditions of each data
198 area. The conditions between the two periods can have the same temperature intensity, as
199 shown in the M09-NH and L10-NH data. However, it can also show that the conditions

before the Samalas eruption were cooler than the post-LIA period (CL11-NH, M05-NH, and J99-NH) or vice versa (M09-AMO and M09-PDO). The M09-AMO data curve shows that the normalized average temperature value in the post-LIA period is almost close to the post-eruption period, this condition is probably related to the location of the M09-AMO data which is close to the eastern Pacific Ocean, an area that is affected by ENSO variations (El Nino-Southern Oscillation). Volcanic events did not significantly cause ENSO or alter ENSO variation (Adams et al. 2003; McGregor et al. 2010). However, the Samalas eruption event is likely to increase the occurrence of moderate to strong El Nino events under prevailing La Nina-like conditions (Alloway et al. 2017).

In this study, the processing of inferential statistics used the Friedman test because the ANOVA test requirements were not accepted. All data are still used at this stage (no data is omitted) because they show the same curve shape, and the results of descriptive statistics are in accordance with the LIA periodization. Based on the processing carried out, the results of the Friedman test show that there is a difference in temperature between the data because the calculated value of the Friedman test (107.87) is greater than the Chi-square table (12.592). The SPSS results also show that the Asymptotic Significance (Asymp Sig) is less than 0.05, which means that there is a difference in temperature between the data (same as the results of manual calculations). Based on these results, to find out data that does not show a temperature difference, the Tukey HSD test can be carried out. The results of the Tukey HSD test in Table 2 show the normalized average temperature values for each data (the results of the Tukey HSD test using SPSS). Decision making refers to the number and results of the table containing the values. The table showing the values shows no difference in temperature between the data (H_0 is accepted and H_1 is rejected). Determination of the data can also be done by manual calculation, namely comparing the HSD value (0.094) with the difference in

the average value between the data (Table 3). Tukey HSD test processing refers to the normalized average temperature value for each data. If the HSD value is greater than the average difference between the data, then there is no difference in temperature and vice versa.

The results obtained from both SPSS processing and manual calculations resulted in 3 groups of data showing no difference in temperature which was presented in the form of a Venn diagram (Figure 4). The results obtained showed that groups 1 and 2 had 3 data with the same temperature effect, but the M09-NH and J99-NH data showed differences because the HSD value was smaller than the normalized average temperature difference between the two data. The Tukey HSD test has a threshold value to determine the relationship between temperature effects and data. The HSD value of 0.094 is the limit to indicate whether there is a temperature difference between the data. The Tukey HSD test compares the HSD value with the difference in the average normalized temperature between the data (one by one). When referring to the HSD values obtained, groups 1 and 2 have 4 data showing no difference in temperature, while group 3 shows 5 data.

Next, curves were formed from the data for each group to show the response of the normalized mean temperature values at 50-year intervals (Figure 5a-5c). The curve results obtained show a similar trend of temperature changes, where the years 1250-1300 showed a decrease in temperature caused by volcanism activity (Brewington 2016). The volcanic activity in question probably originated from the eruptions of Mount Samalas in 1257 (Lavigne et al. 2013) and Mount Quilotoa in 1280 (Muro et al. 2004). The Samalas eruption caused the temperature to drop and freeze suddenly in 1275 (Miller et al. 2012). These conditions can indicate that the impact of the Samalas eruption did not end when the Quilotoa eruption occurred. The effect of the Samalas eruption continues and is getting worse because

it is affected by additional sulfate injection from the Quilotoa eruption in Ecuador (Newhall et al. 2017), as evidenced by the results of the curve that continues to show a decrease in temperature from year to year 1310-1360. Furthermore, in the years 1370-1420, the effect of the eruption began to decrease (experienced an increase in temperature) but had not returned to normal conditions. Then the temperature drops again occurred in 1430-1480, the main cause of the decrease in temperature that occurred was originally thought to have come from the Kuwae eruption in Vanuatu in 1452 (Briffa et al. 1998). However, the yield of these eruptive deposits was too small to be responsible for the spike in H_2SO_4 levels at that time interval. The drop in temperature is probably still related to the two previous eruptions (Samalas and Quilotoa). The climatic conditions after the Kuwae eruption continued to show a significant decrease in temperature, as shown in the trend curve of temperature changes in the period 1430 to 1720. This condition was associated with additional sulfate contributors originating from a series of large eruptions, such as the eruption of Mount Villarica in Chile in February 1640, Mount Komaga in Japan on 31 July 1640 (6 VEI), Mount Parker in the Philippines 1641 (5 VEI) and Long Island in New Guinea 1660 (6 VEI) (Briffa et al. 1998). In 1730-1780, temperature conditions began to recover (increase). However, the Tambora eruption again occurred in Lombok. The Tambora eruption in 1815 was a very powerful eruption (7 VEI) and is known as the year without a summer (Morita et al. 2005; McGregor et al. 2010; Raible et al. 2016). The eruption of Krakatoa (Indonesia) in 1883 (Newhall et al. 2017) also worsened climatic conditions. As a result of several eruptions after the Samalas eruption, climatic conditions continued to decline although there were occasional increases. The cooling did not stop for several years after the Samalas eruption. However, the Samalas eruption that marked the start of the LIA was supported by the additional influence of a large sulfur-rich eruption causing prolonged climate change after the Samalas eruption (Newhall et al. 2017).

Conclusions

The eruption of Samalas initiated climate change that resulted in LIA, as evidenced by the trend of the normalized average temperature change curve at 50-year intervals from 3 data groups in the Northern Hemisphere. The data shows the global climate effect due to the Samalas eruption, as can be seen from the shape of the digital curve with the pattern of changes that are not too different, the results of descriptive statistics according to the LIA periodization, and the results of inferential statistics show that the HSD value (0.094) is greater than the difference in the normalized average temperature value. between data, it means that there is no difference in temperature (H_0 is accepted and H_1 is rejected). The curves of the three data groups show that temperature conditions continue to decline after the Samalas eruption, although sometimes there is an increase but still cannot return to normal conditions. This condition is attributed to the additional influence (sulphate injection) from a series of volcanic eruptions large enough to cause continuous cooling for several years after the Samalas eruption. However, climatic conditions continued to deteriorate and led to a prolonged drop in temperature. Thus, the Samalas eruption in 1257 was not the only eruption that resulted in LIA. However, it initiated climate change which resulted in LIA being supported by other subsequent major eruptions.

CRediT authorship contribution statement

Ika Umratul Asni Aminy: Conceptualization, Formal analysis, Investigation, Methodology, Software, Validation, Writing-original draft, Writing-review & editing. **Satria Bijaksana & Darharta Dahrin**: Conceptualization, Methodology, Supervision, Writing-original draft, Writing-review & editing.

Declaration of Competing Interest

The authors declare that they have no known competing financial interests or personal relationships that could have appeared to influence the work reported in this paper.

References

Abdi H, Williams LJ (2010) Tukey's Honestly Significant Difference (HSD) Test. In: Salkind NJ (Ed) Encyclopedia of Research Design. Sage. Thousand Oaks, California, pp 1-5

Adams JB, Mann ME, Ammann CM (2003) Proxy evidence for an El Niño-like response to volcanic forcing. Nature 426: 274-278

Alloway BV, Andreastuti S, Setiawan R, Miksic J, Hua Q (2017) Archaeological implications of a widespread 13th Century tephra marker across the central Indonesian Archipelago. Quaternary Sci Rev 155: 86-99

Aubry TJ, Staunton-Sykes J, Marshall LR, Haywood J, Abraham NL, Schmidt A (2021) Climate change modulates the stratospheric volcanic sulfate aerosol lifecycle and radiative forcing from tropical eruption. Nat Commun 12: 1-16

Bradley RS, Jones PD (1992) When was the "Little Ice Age"?. In: Mikami T (Ed) Proceedings of the International Symposium on the Little Ice Age Climate. Department of Geography, Tokyo Metropolitan University, Tokyo, pp 1-4

Bradley RS, Jones PD (1993) 'Little Ice Age' summer temperature variations: their nature and relevance to recent global warming trends. Holocene 3: 367-376

Bradley RS (2015) Paleoclimatology: reconstructing climates of the quaternary, third edition. Academic Press, Amsterdam

Brewington SD (2016) The social costs of resilience: an example from the Faroe Islands. Archeol Pap Am Anthropol Assoc 27: 95-105

Briffa K.R, Jones PD, Schweingruber FH, Osborn TJ (1998) Influence of volcanic eruptions on Northern Hemisphere summer temperature over the past 600 years. Nature 393: 450-455

Büntgen U, Smith SH, Wagner S, Krusic P, Esper J, Piermattei A, Crivellaro A, Reinig F, Tegel W, Kirdyanov A, Trnka M, Oppenheimer C (2022) Global tree-ring response and inferred climate variation following the mid-thirteenth century Samalas eruption. Clim Dynam. https://doi.org/10.1007/s00382-022-06141-3

Christiansen B, Ljungqvist FC (2011) Reconstruction of the extratropical NH mean temperature over the last millennium with a method that preserves low-frequency variability. J Climate 24: 6013-6034

Gennaretti F, Arseneault D, Nicault A, Perreault L, Bégin Y (2014) Volcano-induced regime shifts in millennial tree-ring chronologies from northeastern North America. P Natl Acad Sci USA 111: 10077–10082

Hansen J, Lacis AA, Ruedy R, Sato M (1992) Potential climate impact of Mount Pinatubo eruption. Geophys Res Lett 19: 215-218

Jones PD, New M, Parker DE, Martin S, Rigor IG (1999) Surface air temperature and its changes over the past 150 years. Rev Geophys 37: 173-199

Lavigne F, Degeai J-P, Komorowski J-C, Guillet S, Robert V, Lahitte P, Oppenheimer C, Stoffel M, Vidal CM, Surono, Pratomo I, Wassmer P, Hajdas I, Hadmoko DS, Belizal ED (2013) Source of the great A.D. 1257 mystery eruption unveiled, Samalas volcano, Rinjani Volcanic Complex, Indonesia. P Natl Acad Sci USA 110: 16742 - 16747

Ljungqvist FC (2010) A new reconstruction of temperature variability in the extra-tropical Northern Hemisphere during the last two millennia. Geogr Ann A 92A: 339-351

Mann ME, Zhang Z, Rutherford S, Bradley RS, Hughes MK, Shindell D, Ammann C, Faluvegi G, Ni F (2009) Global signatures and dynamical origins of the Little Ice Age and Medieval Climate Anomaly. Science 326: 1256-1260

Matthes FE (1939) Report of committee on glaciers, April 1939. Am Geophys Union 20: 518-523

Matthews JA, Briffa KR (2005) The 'Little Ice Age': re-evaluation of an evolving concept. Geogr Ann A 87A: 17-36

McCormick MP, Thomason LW, Trepte CR (1995) Atmospheric effects of the Mt Pinatubo eruption. Nature 373: 399-404

McGregor S, Timmermann A, Timm O (2010) A unified proxy for ENSO and PDO variability since 1650. Clim Past 6: 1-17

Miller GH, Geirsdóttir Á, Zhong Y, Larsen DJ, Otto-Bliesner BL, Holland MM, Bailey DA, Refsnider KA, Lehman SJ, Southon JR, Anderson C, Björnsson H, Thordarson T (2012) Abrupt onset of the Little Ice Age triggered by volcanism and sustained by sea-ice/ocean feedbacks. Geophys Res Lett 39: 1-5

Moberg A, Sonechkin DM, Holmgren K, Datsenko NM, Karlén W (2005) Highly variable Northern Hemisphere temperatures reconstructed from low- and high-resolution proxy data. Nature 433: 613-617

Morita O, Nakano Y, Murotani K (2005) The impact of the Mt Pinatubo eruption on the climate of the Northern Hemisphere. J Agric Meteorol 60: 657-660

Muro AD, Neri A, Rosi M (2004) Contemporaneous convective and collapsing eruptive dynamics: The transitional regime of explosive eruptions. Geophys Res Lett 31: 1-4

Newhall C, Self S, Robock A (2017) Anticipating future Volcanic Explosivity Index (VEI) 7 eruptions and their chilling impacts. Geosphere 14: 1-32

Olivia M (2018) The Little Ice Age, the climatic background of present-day warming in Europe, Geogr Res Lett 44: 7-13

Paasche Ø, Bakke J (2010) Defining the Little Ice Age. Clim Past Discuss 6: 2159-2175

Raible CC, Brönnimann S, Auchmann R, Brohan P, Frölicher TL, Graf H-F, Jones P, Luterbacher J, Muthers S, Neukom R, Robock A, Self S, Sudrajat A, Timmreck C, Wegmann M (2016) Tambora 1815 as a test case for high impact volcanic eruptions: Earth system effects. Wires Clim Change 7: 569-589

Rampino MR, Self S (1982) Historical eruption of Tambora (1815), Krakatau (1883) and Agung (1963), their stratospheric aerosols, and climatic impact. Quaternary Res 18: 127-143

Table Captions

Table 1. Temperature reconstruction curve data employed in this work.

Table 2. Tukey HSD test results with SPSS based on normalized average temperature value.

Table 3. The results of the difference in the normalized average temperature value between data. The color in the table shows the HSD value (0.094) is greater than the difference in the normalized average temperature value between data, where each color indicates the groups that have the same temperature effect.

TABLE 1

Start Year (AD)	End Year (AD)	Source Proxy Location	Symbol	Reference
500	2000	Northern Hemisphere	M09-NH	Mann et al. (2009)
		North Atlantic AMO region	M09-AMO	
		North Pacific PDO region	M09-PDO	
1	2000	Northern Hemisphere (30° N - 90° N)	L10-NH	Ljungqvist (2010)
1000	2000	Northern Hemisphere	CL11-NH	Christiansen and Ljungqvist (2011)
200	2000	Northern Hemisphere	M05-NH	Moberg et al. (2005)
1000	2000	Northern Hemisphere	J99-NH	Jones et al. (1999)

443 TABLE 2

Tukey HSD				
Location of Proxy Data	N	Normalized Average Temperature Value (°C)		
		1	2	3
M09-NH	101	0.33160		
M05-NH	101	0.37038	0.37038	
L10-NH	101	0.41595	0.41595	0.41595
CL11-NH	101	0.41814	0.41814	0.41814
J99-NH	101		0.45546	0.45546
M09-AMO	101			0.47092
M09-PDO	101			0.49274

444

445

446

447

448

449

450

451

452

453

454

455

456

457

458

459

460 TABLE 3

461

Data	M09-NH	M05-NH	L10-NH	CL11-NH	J99-NH	M09-AMO	M09-PDO
M09-NH	0						
M05-NH	0.039	0					
L10-NH	0.084	0.046	0				
CL11-NH	0.087	0.048	0.002	0			
J99-NH	0.124	0.085	0.039	0.037	0		
M09-AMO	0.139	0.101	0.055	0.053	0.016	0	
M09-PDO	0.161	0.122	0.077	0.075	0.037	0.022	0

462 **Figure Captions**

463

464 Figure 1. The location of the proxy data used in this study refers to 7 curves of temperature
465 reconstruction. The orange square symbol indicates the location of proxy data from
466 areas dominated by oceans, including the North Atlantic AMO (Atlantic
467 Multidecadal Oscillation) region (0° N - 60° N) and the North Pacific PDO (Pacific
468 Decadal Oscillation) region (22.5° N - 57.5° N, 152.5° E – 132 .5° W). While the
469 other 5 data cover a wide area, namely the Northern Hemisphere (without
470 symbols), where four data cover the entire Northern Hemisphere and the rest only
471 cover the area of 30° N - 90° N. The red triangle is the location of Mount Samalas.

472

473 Figure 2. The results of digitizing the curves before (a-g) and after (h-n) are interpolated and
474 normalized. The black dotted line shows the eruption time of Mount Samalas 1257.

475

476 Figure 3. The response of the normalized average temperature value between the LIA
477 periodization and the location of the proxy data is divided into before the Samalas
478 eruption (blue), after the Samalas eruption (green), LIA (cream), and post-LIA
479 (purple). The LIA period is the coldest compared to other periods, then the period
480 after the Samalas eruption caused by climate disturbances due to the injection of
481 volcanic material released. Meanwhile, the period before the Samalas eruption
482 and post-LIA will not show lower conditions than the other two periods (after the
483 Samalas eruption and LIA).

484

485 Figure 4. Inferential statistical results showed the same effect of temperature for 3 data
486 groups, including group 1 consisting of the data M09-NH, M05-NH, L10-NH,

and CL11-NH (green), group 2 consisting of the data M05-NH, L10-NH, CL11-NH, and J99-NH (blue), and group 3 consisting of the data L10-NH, CL11-NH, J99-NH, M09-AMO, and M09-PDO (yellow).

Figure 5. Responses to changes in the normalized average temperature values with 50-year intervals for each data group, (a) group 1 (M09-NH, M05-NH, L10-NH, and CL11-NH), (b) group 2 (M05-NH, L10-NH, CL11-NH, and J99-NH), and (c) group 3 (L10-NH, CL11-NH, J99-NH, M09-AMO, and M09-PDO).

512

513 FIGURE 1

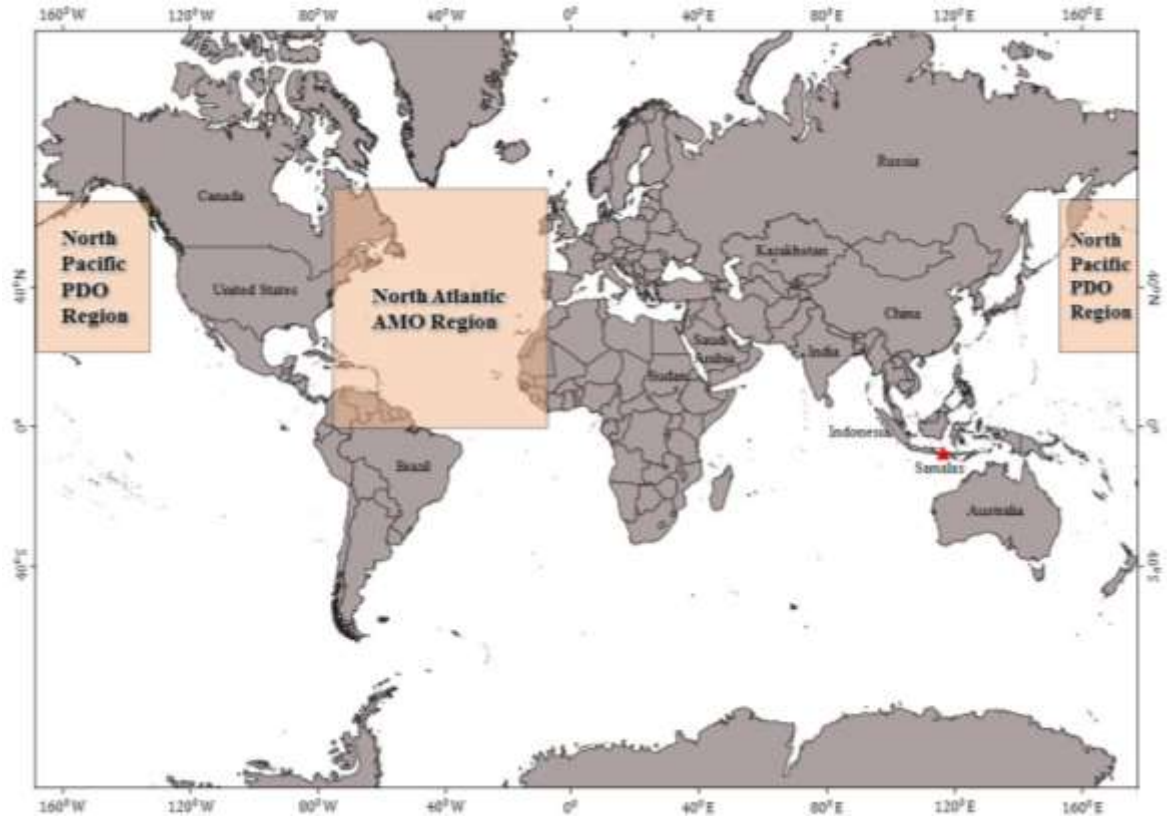

514

FIGURE 2

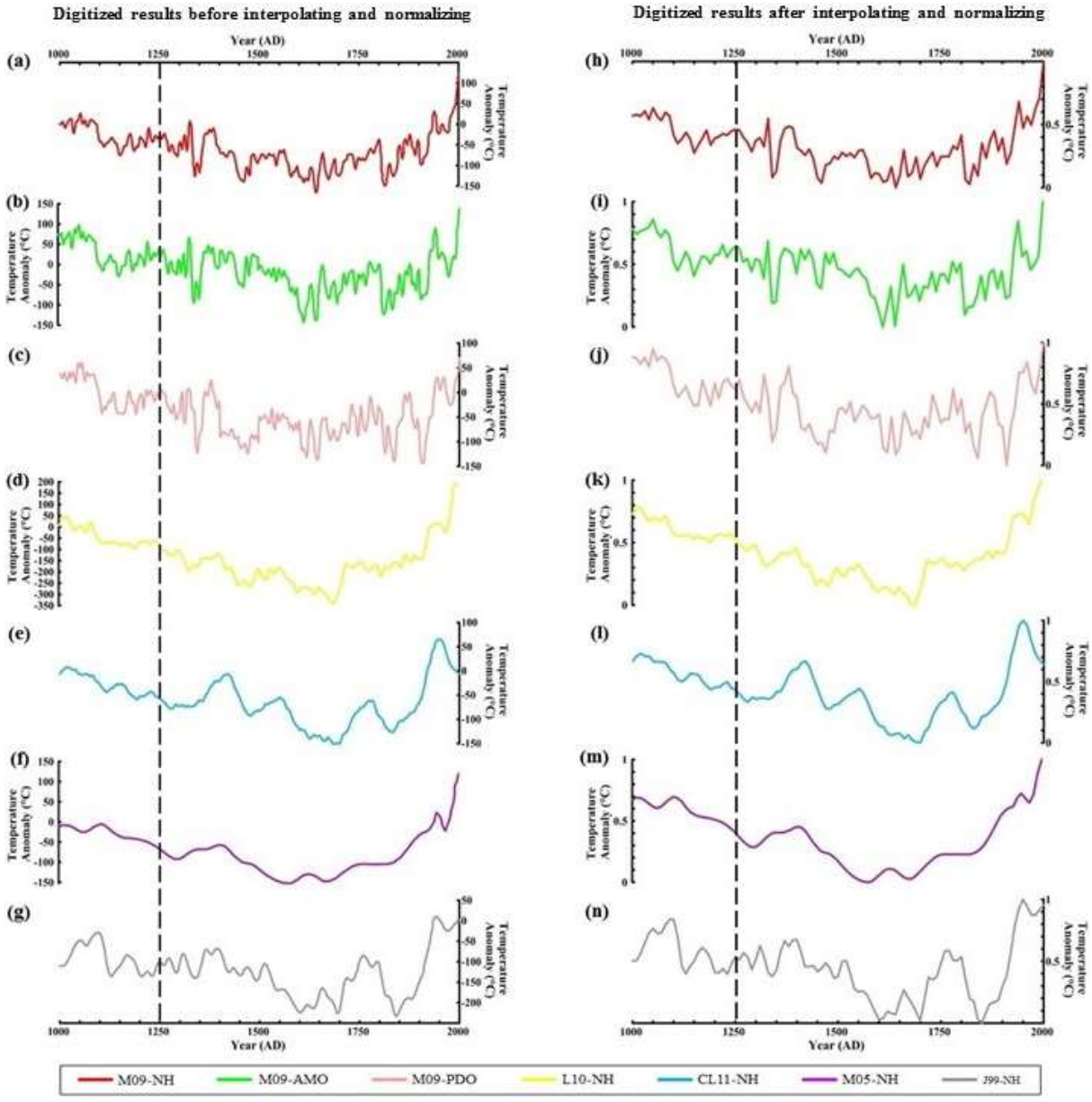
Digitized results before interpolating and normalizing
Digitized results after interpolating and normalizing
Year (AD)
Temperature Anomaly (°C)
(a)
(b)
(c)
(d)
(e)
(f)
(g)
(h)
(i)
(j)
(k)
(l)
(m)
(n)
M09-NH
M09-AMO
M09-PDO
L10-NH
CL11-NH
M05-NH
J99-NH

524 FIGURE 3

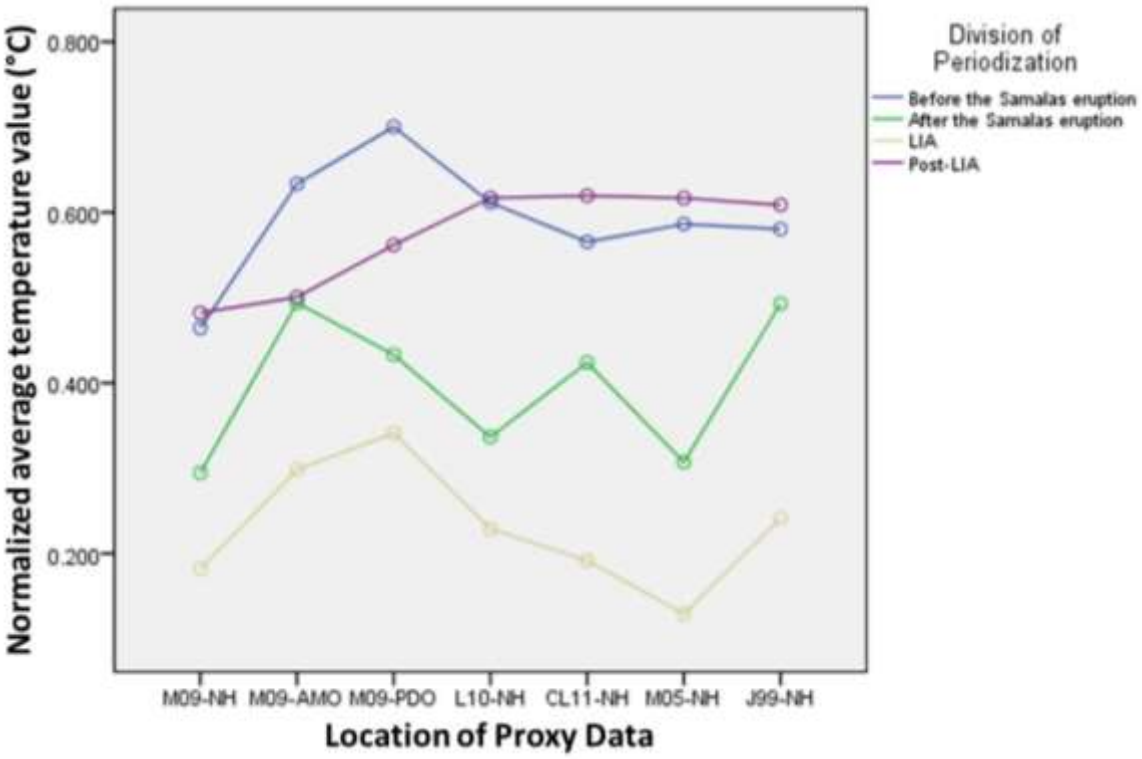

525

526

FIGURE 4

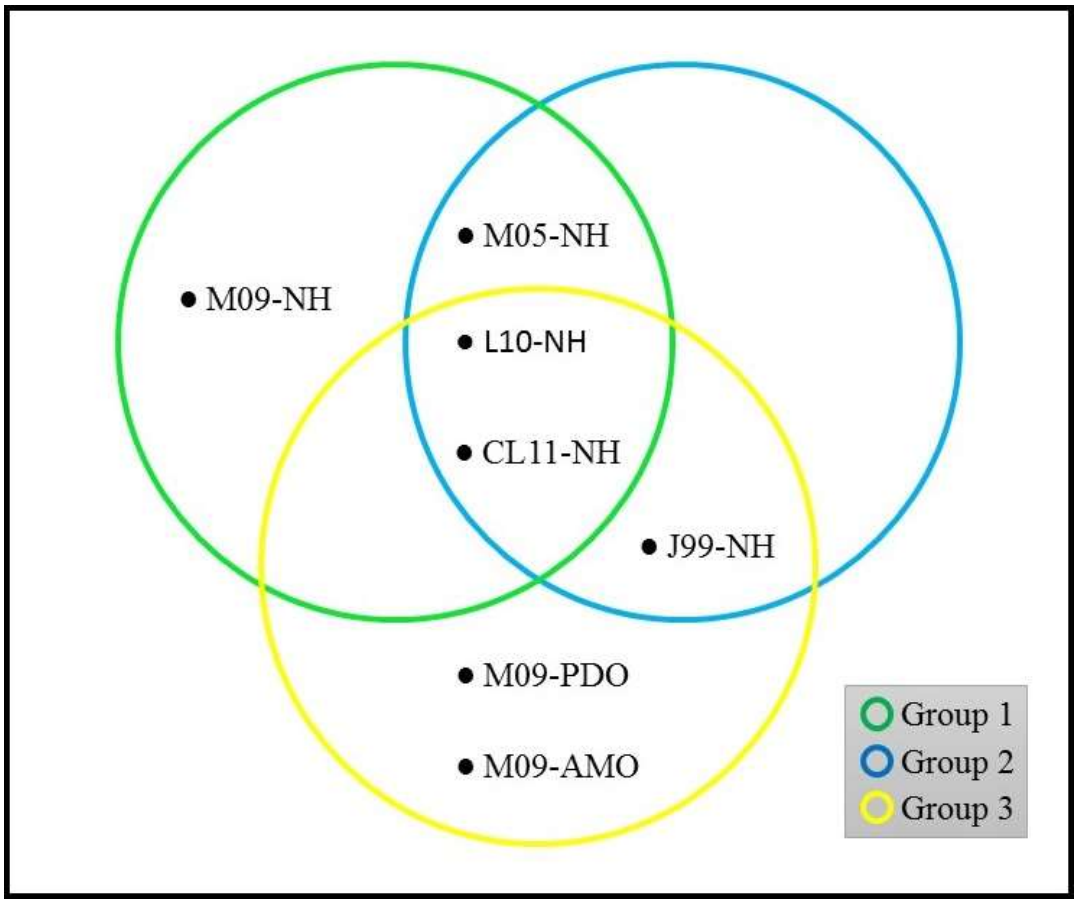
M05-NH
M09-NH
L10-NH
CL11-NH
J99-NH
M09-PDO
M09-AMO
Group 1
Group 2
Group 3

541 FIGURE 5

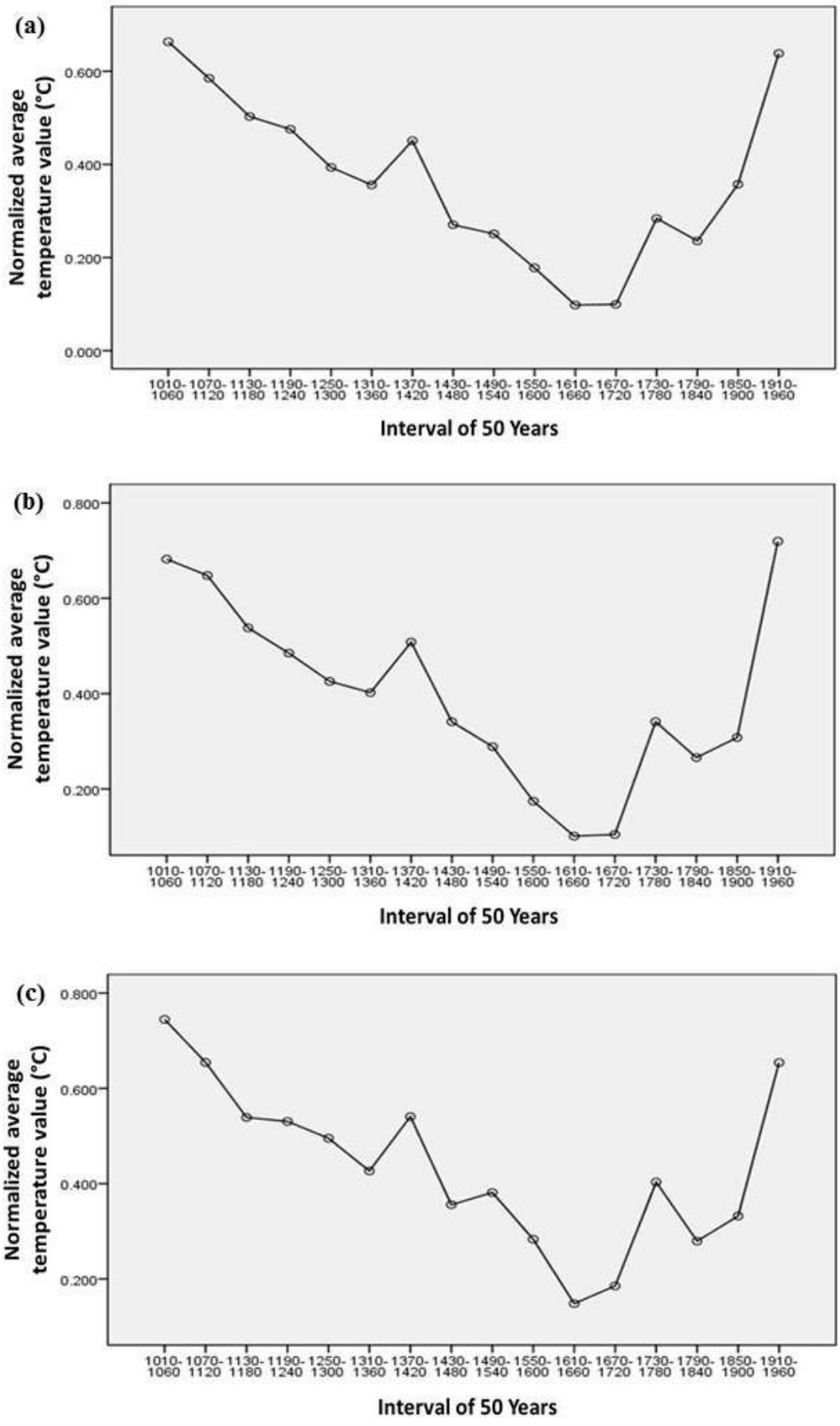

542